chemosensors

Article

Microflow Injection System for Efficient Cu(II) Detection across a Broad Range

David Ricart [1], Antonio David Dorado [1], Conxita Lao-Luque [1] and Mireia Baeza [2,*]

[1] Department of Mining, Industrial and ICT Engineering, Escola Politècnica Superior d'Enginyeria de Manresa, Universitat Politècnica de Catalunya, Avinguda de les Bases de Manresa 61-73, 08240 Manresa, Spain; david.ricart.fort@upc.edu (D.R.); toni.dorado@upc.edu (A.D.D.); conxita.lao@upc.edu (C.L.-L.)
[2] GENOCOV Research Group, Department of Chemistry, Faculty of Science, Edifici C-Nord, Universitat Autònoma de Barcelona, Carrer dels Til·lers, 08193 Bellaterra, Spain
* Correspondence: mariadelmar.baeza@uab.cat

Abstract: In this study, a modular, multi-step, photometric microflow injection analysis (micro-FIA) system for the automatic determination of Cu(II) in a bioreactor was developed. The system incorporates diverse 3D-printed modules, including a platform formed by a mixer module to mix Cu(II) with hydroxylamine, which reduces Cu(II) to Cu(I) linked to a diluter module via a Tesla valve, a chelation mixer module, a disperser module, and a detector module provided by an LED light source at λ = 455 nm and a light dependence resistor (LDR) as a light intensity detector. The system measures the color intensity resulting from the chelation between Cu(I) and neocuproine. The micro-FIA system demonstrated good capability for automatic and continuous Cu(II) determination, in a wide range of Cu concentrations, from 34 to 2000 mg L^{-1}. The device exhibits a good repeatability (coefficient of variation below 2% across the measured concentration range), good reproducibility, and has an accuracy of around 100% between 600 and 1900 mg L^{-1}. Real samples were analyzed using both the micro-FIA system and an atomic absorption spectroscopy method, revealing no statistically significant differences. Additionally, a Tesla valve located before the detector substituted a 3-way solenoid valve, eliminating the need for moving parts.

Keywords: Cu(II); 3D-printed microfluidic platform; micro-FIA; bioleaching; e-waste; circular economy

check for updates

Citation: Ricart, D.; Dorado, A.D.; Lao-Luque, C.; Baeza, M. Microflow Injection System for Efficient Cu(II) Detection across a Broad Range. *Chemosensors* **2024**, *12*, 119. https://doi.org/10.3390/chemosensors12070119

Received: 22 May 2024
Revised: 19 June 2024
Accepted: 24 June 2024
Published: 29 June 2024

Correction Statement: This article has been republished with a minor change. The change does not affect the scientific content of the article and further details are available within the backmatter of the website version of this article.

Copyright: © 2024 by the authors. Licensee MDPI, Basel, Switzerland. This article is an open access article distributed under the terms and conditions of the Creative Commons Attribution (CC BY) license (https://creativecommons.org/licenses/by/4.0/).

1. Introduction

The exponential growth of electronic waste (e-waste) in the past few decades, driven by rapid technological advancements and planned obsolescence, has become a pressing global concern. According to the World Health Organization (WHO) [1], e-waste generation has increased by 3–5% annually. This escalating issue necessitates the development of effective e-waste recycling methods, not only to address environmental concerns but also due to the presence in this e-waste of valuable metals like copper, silver, cobalt, lithium, gold, and nickel. The recovery of these metals from e-waste holds immense economic potential for various new applications.

Nevertheless, the intricate composition of e-waste, consisting of a complex amalgamation of organic materials, ceramics, and metals, poses significant challenges in the recycling process. The predominant methods employed for metal recovery from e-waste, namely pyrometallurgical and hydrometallurgical processes, incur substantial expense and exert a considerable environmental toll due to their reliance on high temperatures and harsh chemicals. In recent years, alternative recycling technologies that prioritize environmental sustainability have garnered attention. One such approach is bioleaching, which harnesses the activity of specific microorganisms to generate leaching agents capable of extracting metals. Although bioleaching has found success in the mining industry for low-grade ores [2], such as in commercial bio-heap processes [3,4], its potential for large-scale metal recovery from e-waste [5,6] is currently under exploration.

The bioleaching of copper from electronic waste utilizing *Acidithiobacillus ferrooxidans* has been established as a promising approach [2–6], leveraging the bacteria's ability to facilitate the oxidation of Fe(II) to Fe(III) under acidic conditions. Fe(III) oxidizes the copper present in the residue to its soluble form Cu(II), while it is reduced to Fe(II). This unique capability enables the continuous process of re-oxidizing Fe(II) to Fe(III), establishing a bioleaching cyclic process [7]. The copper bioleaching process typically encompasses two distinct stages. Initially, the oxidation process takes place within a specialized bioreactor, where microorganisms catalyze the conversion of Fe(II) to Fe(III). Subsequently, the Fe(III) solution, devoid of bacteria, is introduced into a separate reactor containing the e-waste, facilitating the extraction of Cu(II). Accurate control of the Cu(II) concentration during the copper extraction stage is crucial for optimizing the bioleaching process.

At present, several methods can determine Cu(II) or total Cu, such as fluorescence [8,9], electroanalytical techniques [10–15], potentiometry with ion-selective electrodes [16,17], atomic absorption spectrometry [18–20], inductively coupled plasma mass spectrometry (ICP-MS) [21], paper-based microfluidic analytical devices [22], atomic fluorescence spectrometry [23], high-performance liquid chromatography [24], mass spectrometry [25], and colorimetric and UV-Vis spectrometry [26–43]. However, these conventional approaches suffer from inherent limitations, such as their labor-intensive nature, lack of automation, dependence on skilled personnel, strict laboratory conditions, and the need for extensive sample preparation, all of which contribute to increased analysis time and potential compromise in the quality of data analysis. Another drawback is the limited dynamic range response of these methods, necessitating substantial dilutions for the analysis of high-concentration samples. This poses a significant challenge when quantifying Cu(II) in a bioreactor, where concentrations can reach as high as 3000 mg L^{-1}.

In this sense, the implementation of flow injection analysis (FIA) offers a versatile approach for the monitoring of diverse parameters, such as Cu ions, across complex matrices [44,45]. FIA methods enable real-time and in situ analysis, facilitating automation and enabling high sample throughput. Despite these advantages, there is a noticeable dearth of published research on the application of FIA for monitoring high Cu(II) concentrations in bioreactors. To bridge this research gap, FIA based on microfluidic platforms fabricated through 3D printing presents a promising solution. This approach offers a high degree of customization and accessibility through the use of computer-aided design (CAD) programs.

The usual detection method is colorimetry, which utilizes a chelating agent to complex with metallic cations, resulting in a colored product. Different chelating agents have been used in the literature. Cuprone allows for direct Cu(II) determination, but it suffers from interferences with other metal ions [34,35]. However, Cu(II) can be determined by reducing it to Cu(I), which has the three specific chelators neocuproine, cuproine, and bathocuproine [26,28–33] without interference from other ions or species present in the medium.

The main aim of this study is to establish a reliable and versatile microflow injection analysis (micro-FIA) system that is fully automated and integrated, to effectively monitor and quantify high concentrations of Cu(II) in a bioreactor. The detection of Cu(II) was achieved by implementing a reduction of Cu(II) to Cu(I), followed by the formation of a selective colored complex between Cu(I) and neocuproine, which exhibits an absorption peak at 454 nm [30]. The design of a micro-FIA analyzer was accomplished using computer-aided design (CAD) software (Version S.51.0.0, 2022), incorporating narrow microchannels that minimize sample and reagent volumes. These design features will not only contribute to cost savings but also facilitate frequent analyses, enabling real-time determination of Cu(II) concentrations to ensure precise and accurate results.

2. Materials and Methods

2.1. Chemicals and Reagents

In this study, a black, 1.75 mm polylactic acid (PLA) filament was used (LEON 3D, Valverde de la Virgen, Spain). $CuSO_4 \cdot 5H_2O$ (99%) was obtained from Labkem (Barcelona,

Spain), neocuproine hemihydrate (98+%) from Thermoscientfic (Barcelona, Spain), ethanol (96%) from Scharlau (Polinya, Spain), H_2SO_4 (95–98%) from Panreac (Castellar del Vallès, Spain), sodium acetate (99+%) from T3Q (Sentmenat, Spain), and hydroxylamine hydrochloride (98%) from Panreac (Castellar del Vallès, Spain). All chemicals utilized in this study were of analytical reagent grade.

A pH = 2, aqueous acidic solution was prepared by dissolving H_2SO_4 in deionized water. This pH was chosen to match the operating conditions of the bioreactor. A 6000 mg L^{-1} stock solution of Cu(II) was prepared by dissolving $CuSO_4 \cdot 5H_2O$ in aqueous acidic solution at pH = 2. The hydroxylamine solution 10% (*w*/*v*) was prepared by dissolving hydroxylamine in aqueous acidic solution at pH = 2 [46]. The acetate solution 0.003 M was prepared by dissolving sodium acetate in deionized water.

A 0.15% (*w*/*v*) neocuproine solution in 20% (*v*/*v*) ethanol was prepared by first dissolving neocuproine in ethanol, followed by the addition of deionized water. Higher neocuproine concentrations exhibited instability, precipitating as needle-shaped crystals. Otherwise, increasing the ethanol concentration compromised miscibility with water, leading to suboptimal signal quality due to refractive index mismatch.

All solutions were prepared with deionized water for a Milli-Q system (Millipore, Billerica, MA, USA).

2.2. Microfluidic 3D Platform and Module Design, Printing Conditions, and Fabrication

The CAD model design for all the modules and platforms was created using AutoCAD 2022, version S.51.0.0 (copyright © 2021 Autodesk, Inc.). The manufacture of the pieces was carried out using a Prusa i3MK3S+ printer (Prusa Research Prague, Czech Republic). The CAD of platform 1, formed by two modules (mixer and diluter) connected via a Tesla valve, is shown in Figure S1. Platform 2 is a mixer with a height of 1 mm, which has the same design as that presented in this work [47]. Platform 3, formed by a disperser and a Tesla valve, is shown in Figure S2.

PLA was chosen as the material for printing the modular blocks due to it being affordable and user- and eco-friendly. The CAD models were exported as stereolithography (STL) files and opened in CURA 4.12.1 software. The printing settings were configured within this software environment. Subsequently, CURA generated a G-code file containing the instructions and information necessary for printing the platforms.

The printing conditions for the height layers were set as the following: the layer height was set to 0.1 mm and the initial layer height to 0.2 mm. The wall line count was set to 8, and a retraction distance of 1.6 mm was used. The line width was set to 0.2 mm, and the top/bottom thickness was set to 1 mm. Additionally, 10 bottom and top layers were applied, with the initial printing temperature set to 215 °C and subsequently reduced to 200 °C. The temperature of the printer plate was set to 60 °C. During the CAD design process, it was determined that 4–5 mm separation between the channel and the external wall was sufficient.

2.3. Experimental Setup

The overall configuration of the micro-FIA system is illustrated in Figure 1 showing its key components: (i) the injection system; (ii) the assembled 3D-printed platforms; and (iii) the data acquisition system. Fluid flow was managed by two peristaltic pumps (a and b).

To pump the carrier, reactant, and diluent, a peristaltic pump, Hyiafex HF-LabV1-III/AMC12(10) from HYGIAFLEX (L'Hospitalet de Llobregat, Barcelona), equipped with 2 mm internal diameter tubing silicon from HYGIAFLEX (L'Hospitalet de Llobregat, Barcelona), was used. A six-way injection valve manufactured by Hamilton Injector MVP (Cary, NC, USA) was used for sample injection. To fill the loop sample and clean the detector, a GILSON Minipuls 3 R4 with a 4-channel head and (Gilson, Villiers-le-Bel, France) peristaltic pump equipped with 1.52 mm internal diameter Tygon®tubing (Ismatec) was used. The ethanol was introduced to the system through a 3D-printed Tesla valve

design for this proposed in platform 3. The tubes used to connect to the six-way injection valve were polytetrafluoroethylene (PTFE) (Tecator, Hoganas, Sweden), with a 0.8 mm internal diameter, the sample loop was made with perfluoroalkoxy alkanes (PFAs) (VWR, Llinars del Vallés, Barcelona) with a 0.5 mm internal diameter.

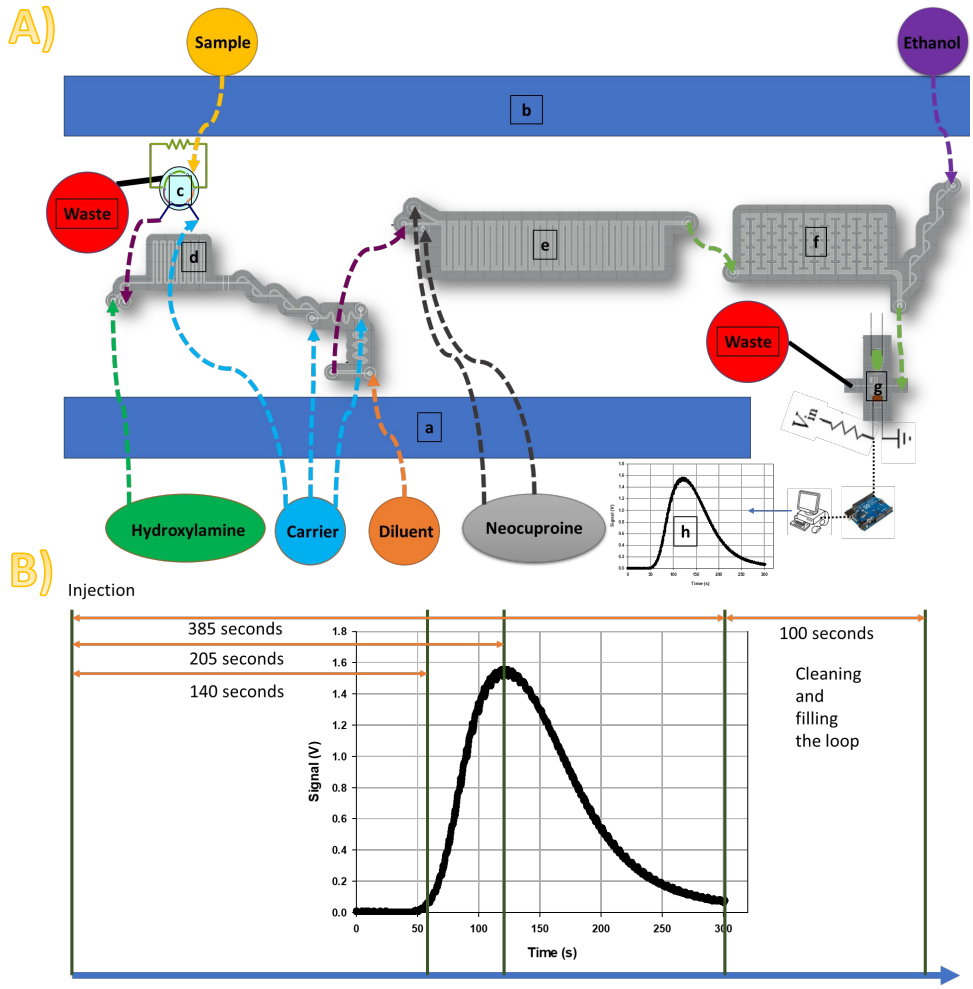

Figure 1. (**A**) Micro-FIA system diagram to determine Cu(II). (**a**) Peristaltic pump for diluent, carrier, and reagent; (**b**) peristaltic pump for ethanol and sample; (**c**) six-way injection valve; (**d**) platform 1 for copper reduction and dilution by adding diluent; (**e**) platform 2 for neocuproine reaction; (**f**) platform 3 for complex dilution by dispersion; (**g**) detector; and (**h**) analytical signal, the peak height is proportional to Cu(II) concentration. (**B**) Diagram and sequences of time to analytical signals.

The experimental operational parameters were fixed as follows. The injection volume (Figure 1c) was 25 µL; the volume of platform 1 including the mixer connected through a Tesla valve with a diluter (Figure 1d) was 363 mm^3; platform 2 was only a mixer (Figure 1e); and the volumes of platform 3, which was a disperser that included another Tesla valve (Figure 1f), were 2034 mm^3 and 1685 mm^3, respectively. The flow rate of solutions was between 0.20 mL min^{-1} and 0.39 mL min^{-1}:hydroxylamine 10% w/v at 0.20 mL min^{-1}, the carrier was a solution at pH = 2 by H_2SO_4 at 0.24 mL min^{-1}, and the diluent was a solution of sodium acetate 0.003 M at 0.24 mL min^{-1} and neocuproine at 0.15% in 20% v/v ethanol:water at 0.27 mL min^{-1}. The flow rate of ethanol 96% was 0.39 mL min^{-1}.

The detection system integrated mainly two elements, a light-emitting diode (LED) (OSB3SA5111A; Transfer Multisort Elektronik, Łódź, Poland), emitting light in the wavelength range of 455 nm, and a light-dependent resistor (LDR) (PGM5537; Transfer Multisort Elektronik, Poland).

The 3D-printed modules of the micro-FIA system were connected using polyvinyl chloride (PVC) tubes of variable length and 1.52 mm internal diameter Tygon®tubing (Ismatec) (Figure 1A). The inlet/outlet 3D modules were designed as described in a previous study [47].

The system's analytical response is depicted in Figure 1B, where the peak height is directly proportional to the concentration of Cu(II).

2.4. 3D Optical Flow Cell Detector

The detector was designed based on previous studies [47] and its operational principles remain identical. This detector is capable of determining the concentrations of copper, converting light intensity into a proportional electrical signal (mV), and the signal was collected at a rate of 0.1 s. The detector consisted of an LDR of 5 mm in diameter and an LED emitting at 455 nm. The LED was powered by 3 volts and 20 mA. For the purpose of data acquisition, the LDR was connected to an Arduino UNO and integrated into a voltage divider circuit powered by 5V. In the voltage divider circuit, a 10 kΩ resistance was placed first, followed by the LDR whose resistance decreased as the intensity of light increased. This configuration made the measured voltage directly proportional to the absorbance. The voltage was then sent to the computer by the Arduino every 100 ms. The only differences were in the CAD design. The internal diameter of the inlets was 1 mm, the channels measured 1 mm in height and 1 mm in width, and the flow cell measured 2 mm in diameter. These changes were implemented to facilitate the flow path and to prevent overpressure. Another modification involved substituting the rectangular supports with cradle-shaped supports, thus eliminating the necessity to employ a flat screwdriver for support removal after printing was completed.

2.5. Micro-FIA Procedure for Copper Determination

The analysis cycle operated in the following manner: Initially, a peristaltic pump (Figure 1b) was used to pump the sample into a six-way valve, set in load mode (Figure 1c), filling the sample loop (25 µL). Next, the pump stopped, the six-way valve was changed into an injection position and a second peristaltic pump (Figure 1a) was activated to pump reagents (hydroxylamine 10% w/v), diluent (sodium acetate 0.003 M), and carrier (solution at pH = 2 by H_2SO_4) into the system. Subsequently, the sample was introduced to platform 1 (Figure 1d), where Cu(II) was reduced to Cu(I) by hydroxylamine since neocuproine specifically reacts with Cu(I) [26,28–33].

As the sample was a suspension from the bioleaching reactor possibly containing high concentrations of Cu(II) (up to 3000 mg L^{-1}), it was directed towards the diluter module using a Tesla valve in the platform 1 (Figure 1d) to prevent any backflow. The purpose of the diluter was to adjust the Cu(II) concentrations within a measurable operational range. The diluted sample with Cu(I) then entered platform 2, which was only a mixer module (Figure 1e), where it reacted with the chelating reagent (0.15% w/v of neocuproine), resulting in an orange color complex whose intensity was directly proportional to the Cu(I) concentration.

The mixture then passed through the disperser module in platform 3 (Figure 1f). The disperser was incorporated into the system to dilute the Cu(I)–neocuproine complex by dispersion and decrease the peak height preventing the signal saturation of the detector. Afterwards, the sample entered the 3D optical flow cell (Figure 1g) where the absorbance of the Cu(I) complex was measured and transformed into electrical signals represented by peak height (mV) (Figure 1h). Finally, the solution was released from the system as waste and the pump was turned off (Figure 1a).

After each measurement, the detector was cleaned to ensure accurate subsequent readings. This cleaning process involved activating the first pump (Figure 1b), which pumped ethanol through the Tesla valve. This valve type has several advantages over a solenoid valve, such as a customizable design, longer lifespan, and the absence of moving parts. In this step, the sample loop was filled again for the next measurement.

To control the system, a custom software application was created using LabVIEW 2021. This software was specifically designed to manage the functionality of the 6-way valve through serial communication RS-232. To establish communication with the Arduino UNO, LINX, a software package was installed within LabVIEW. The Arduino UNO was responsible for measuring the voltage at the voltage divider and LabVIEW then processed these signals to determine the peak height and thus the concentration of copper in the sample. Additionally, Arduino UNO was connected to a Relay Shield 3.0 from Seeed Studio, enabling it to send signals to operate the pumps.

2.6. Spiked and Real Samples

Several real samples were subjected to analysis to validate the functionality of the analyzer. These included medium samples from a bioleaching reactor, water samples from a nearby reservoir (Parc de l'Agulla, Manresa, Spain), leachate obtained from the acidic digestion of electric scooter batteries, and residual solutions from copper electrodeposition processes. All samples were filtered using a Millipore cellulose acetate syringe filter of 0.45 µm (Chemlab group, Terrassa, Spain) before analysis. The samples were analyzed in triplicate, after the addition of a known concentration of Cu(II).

The samples obtained from copper electrodeposition were diluted using an acidic solution at dilution factors of 1/3, 1/2, and 2/3. From each dilution, two separate aliquots were taken. One aliquot was analyzed directly, while in the other aliquot, 500 mg L^{-1} Cu(II) was added and then analyzed. The analysis was performed in triplicate.

The results obtained from the micro-FIA system were compared with the standard method using atomic absorption spectroscopy (PinAAcle 500; PerkinElmer, Waltham, MA, USA).

3. Results and Discussion

3.1. Design and Optimization of Passive Elements

To maximize the effectiveness of the micro-FIA device outlined in the experimental section, various operational parameters were explored to achieve optimal performance. The main objectives of the design were to extend the dynamic range for copper analysis, enhance the mixing efficiency within the analyzer, and improve the stability of the detector, and accordingly, the precision of the method.

Platform 1 (Figure 1d) consisted of three elements: (1) the reactor for the Cu(II) reduction with hydroxylamine; (2) the Tesla valve to prevent the carrier backflow; and (3) the diluter.

Platform 1: hydroxylamine mixer. Within the mixer's reactor, the chemical reaction between the sample and the reducing agent resulting in the reduction of Cu(II) to Cu(I) took place. The design of the reactor, as presented in Figure S1A,B, incorporated two inlets. One entrance was used for introducing the sample, while the other allowed the entry of hydroxylamine. Both inlets measured 0.51 mm in internal diameter. The reactor channel was designed with a combination of linear segments and square turns to enhance the efficiency of mixing [48]. This design culminated in the Tesla valve, which was incorporated to prevent liquid backflow.

The channels were designed with a height of 0.5 mm and a width of 0.75 mm, and they were seamlessly connected to the reagent channel at a T-junction. Within the mixer, a designated mixing zone (Figure S1B) allowed sufficient time for the complete reaction between the sample and the reagent, enabling the neocuproine to effectively interact with Cu(I) in its copper form. To achieve optimal mixing efficiency, the mixer incorporated a total of 28 90-degree turns. Each turn measured 24 mm in length and 2.85 mm in width, creating flow turbulence within the channel to facilitate thorough sample mixing.

Platform 1: Tesla valve. This passive valve, originally designed by Nikola Tesla [49], was a fluid flow control device that operated on a unique principle without any moving parts. It employed a series of specially designed channels to regulate the flow of fluid in a unidirectional manner, creating greater resistance to flow in one direction compared

to the opposite direction. This valve is renowned for its simplicity, efficiency, and low maintenance requirements, and its innovative design has made it a popular choice for fluid control in various engineering applications.

The shape of the Tesla valve (Figure 2) was carefully selected based on mathematical analysis, which demonstrated that it achieved a greater pressure drop in the reverse flow [50]. This specific valve shape was chosen to prevent backflow between the hydroxylamine mixer (on platform 1) and the diluter modules (as illustrated in Figure S1A). The Tesla valve has a height of 0.75 mm, featuring a gradual increase in the channel connecting the mixer and the valve.

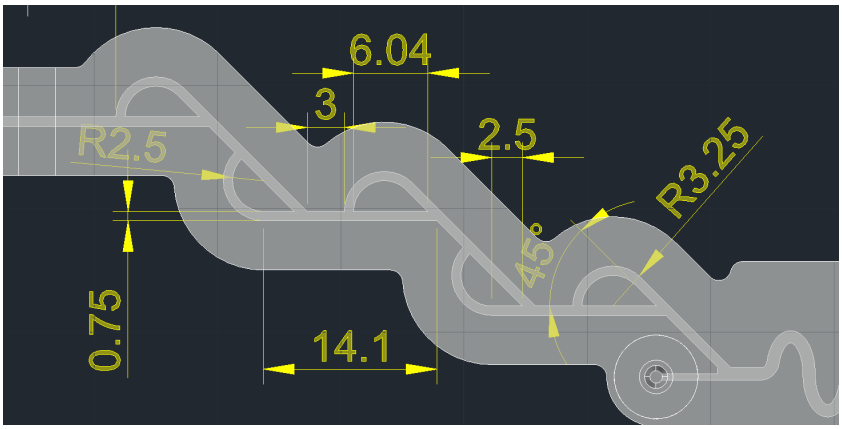

Figure 2. Dimensional labeling of the Tesla valve in CAD. The units for the dimensions are in millimeters.

Platform 1: diluter. The diluter module played a crucial role in adjusting the sample concentration in the linear response range of the micro-FIA analyzer. Given the anticipated high Cu(II) concentrations in samples from the bioleaching reactor, which could reach up to 3000 mg L^{-1} of Cu(II), the dilution step was very important [5]. The design of the diluter, including the diameters of the inlets, outlets, and channels, was carefully considered to facilitate the proper flow of the reaction mixture.

To enhance the dilution process and prevent excessive pressure in the diluter module, a three-point dilution strategy was employed. The diluter's main channel was divided into two serpentine sections and a straight segment. In each succeeding segment, the internal width of the main channel was increased by 0.5 mm. The size of the sections was carefully picked. The first portion was established to be 43 mm long and 1 mm wide, the second to be 67 mm long and 1.5 mm wide, and the last one 17 mm long and 2 mm wide. Rectangular channels with dimensions of 0.5 mm in width, 0.75 mm in height, and 4 mm in length were used to create the inlet connections. The inlet and outlet diameter dimensions were determined to be 1 mm and 1.5 mm, respectively (Figure S1C).

Platform 2. The reaction between Cu(I) and neocuproine occurred in the mixer, forming an orange chelate that absorbed light at 454 nm. The concentration of copper was directly proportional to the measured absorbance. The reactor included three inlets, with one entrance for introducing the diluted sample while the remaining two entrances were used to introduce the reagent, allowing for an increased reagent ratio. The design and characteristics of this module were described previously [47].

Platform 3: disperser with a Tesla valve. The integration of the disperser module was a pivotal advancement in the micro-FIA system's design [47]. It played a vital role in enhancing the dispersion of the chelate, leading to a notable reduction in the signal peak height and in the prevention of detector signal saturation. Positioned between the mixing module (Figure 1e) and the 3D optical microflow cell (Figure 1g), the disperser module featured a main channel with a serpentine shape and additional smaller serpentine segments (Figure 1f). This specific configuration effectively amplified turbulence and facilitated superior dispersion of the colored complex obtained before the detection step. The dimensions were carefully selected to minimize any overpressure issues at the output,

with a width of 2 mm and a height of 1 mm, while the inlet and outlet were designed with diameters of 1.5 mm and 2 mm, respectively. For more detailed insights into the design specifics of the disperser module, refer to Figure S2.

Furthermore, a Tesla valve was located at the outlet. This valve enabled the introduction of ethanol for detector cleaning, eliminating the need for an active 3-way electro-valve and preventing flow in the opposite direction. This integration of a Tesla valve on the disperser ensured efficient detector maintenance.

3.2. Optimization of Operational Conditions

The complete design and optimization of a detector response and characterization was described in previous work [47]. The baseline obtained was stable while the sample was simultaneously diluting and reacting with reactants in the system.

Among the most widely used chelating agents are neocuproine, cuproine, and bathocuproine. They all exhibit similar water solubility, high selectivity, and strong affinity for Cu(I), forming stable complexes [31–33]. A molar extinction coefficient is a key factor in differentiating these chelating agents. A lower molar extinction coefficient allows for a wider linear response range in Cu(II) analysis. This means being able to quantify a broader range of Cu(II) concentrations while maintaining reliable absorbance measurements. Bathocuproine has the highest molar extinction coefficient [32], while neocuproine and cuproine have very similar values [31,33]. Price is the final deciding factor, with neocuproine being the most cost-effective option. Consequently, the target analyte was quantified by measuring the signal produced from the formation of a chelate complex between Cu(I) and neocuproine.

The magnitude of the signal, which is a voltage, was directly proportional to the concentration of Cu(II) present in the sample. Detection of the signal was accomplished using an LDR positioned within a 3D optical microflow cell. Signal processing was carried out by an Arduino microcontroller, and the resulting output signal was then transmitted to a computer for subsequent data analysis. The maximum voltage it could measure was about 4 volts, as 1 volt is where the baseline usually is. Total analysis and cleaning time were between 9 min. To avoid the formation of bubbles that would interfere in the measurements, all solutions were previously sonicated.

3.3. Validation of Microanalyzer Performance

To establish the microanalyzer's suitability, reliability, and robustness in the ongoing assessment of copper concentration within a bioleaching reactor, a process of validation for micro-FIA was made. The key parameters evaluated were the limit of detection (LoD), limit of quantification (LoQ), linear response range, real sample analysis, precision (repeatability and reproducibility), and accuracy.

3.3.1. Precision

Repeatability

The repeatability of the method was evaluated by analyzing two Cu(II) standard solutions of 500 and 1500 mg L^{-1}, six times each, on the same day. The mean, standard deviation, and experimental coefficient of variation (CV) were calculated for each concentration. The Horwitz coefficient (C_{vh}) [51] defines the maximum acceptable CV based on the analyte concentration (g mL^{-1}). This relationship is expressed by the equation: $C_{vh} = 2^{(1-0.5 \cdot \log(C))}$. Table S1 presents the analytical results for each concentration. The experimental CV was less than 2% and lower than the corresponding C_{vh} value for both concentrations. This indicates acceptable repeatability for the method.

Reproducibility

A wide range of Cu(II) concentrations (50, 500, 1000, 1500, and 2000 mg L^{-1}) was used to determine the reproducibility. Each concentration was analyzed three times on four separate days (n = 12) (Figure 3A). The mean, standard deviation, and experimental CV were calculated for each concentration. The experimental CV obtained was compared to the

acceptable limit of C_{vh}. Table S2 summarizes the results. The experimental CV remained less than the C_{vh} across the entire range of concentrations. Consequently, the CV values obtained were considered satisfactory, demonstrating the method's reproducibility.

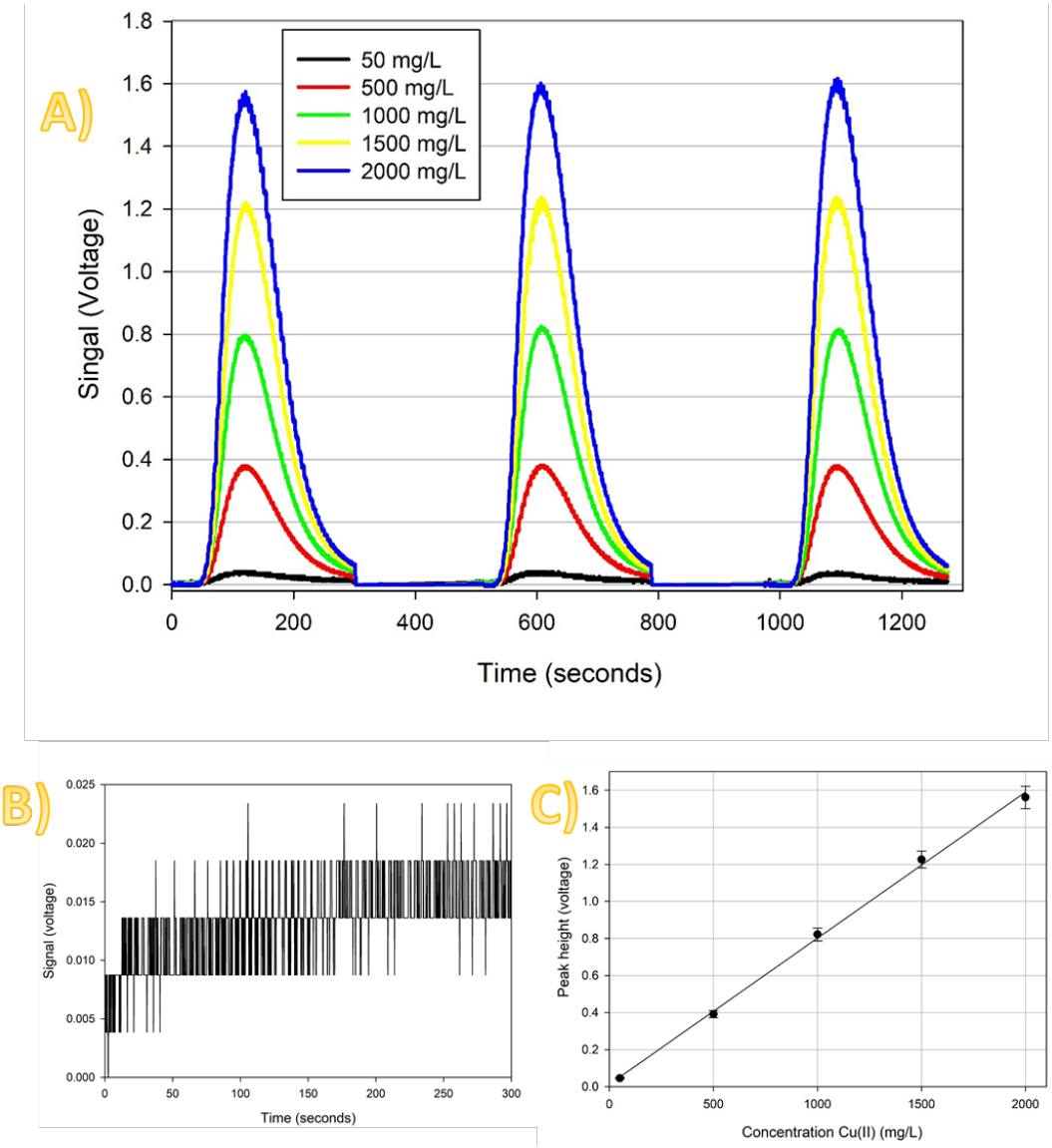

Figure 3. Calibration performed of Cu(II) in the micro-FIA under optimal conditions. (**A**) Analytical signal (λ = 455 nm) at different concentrations; (**B**) blank; and (**C**) calibration plot. The equation of the calibration curve is Peak height (V) = 0.00079 ± 0.00002 [Cu(II)] + 0.01 ± 0.02 (R^2 = 0.998; n = 5 by triplicate).

3.3.2. Limit of Detection and Limit of Quantification

The determination of the limit of detection (LoD) and limit of quantification (LoQ) followed the signal-to-noise approach, a methodology employed in analytical procedures characterized by inherent baseline noise. The signal-to-noise ratio was established through the analysis of the signal of a blank sample. To compute the LoD and LoQ, a series of 200 measurements of the baseline from blanks were performed. Subsequently, the mean and standard deviation values were calculated according to the method outlined [52]. The LoD was derived using the formula, (X + 3Sb)/S, where X represents the mean of the blank measured, Sb is the standard deviation of the blank mean, and S is the slope of the calibration curve or sensitivity. Similarly, the LoQ was determined by employing the equation (X + 10Sb)/S. From employing this methodology, we determined the LoD to be

9 mg L^{-1} and the LoQ to be 34 mg L^{-1}. A representation of the baseline and blank signal is presented in Figure 3B.

3.3.3. Linear Response Range

The linearity of the analytical method assessed the relationship between the analyte concentration and the corresponding peak height expressed in volts. The linear response range spanned from the LoQ to the upper concentration of the linear range. In this study, linearity was determined by analyzing five different Cu(II) standard solutions in triplicate, with concentrations ranging from 34 to 2000 mg L^{-1}. The obtained results were used to create a calibration plot using the least squares method, yielding a high coefficient of determination (R^2) of 0.998. This indicated a strong linear correlation between the analyte concentration and the signal response within the pH range of 1.9 to 2.1. The equation of the calibration curve (Figure 3C) is Peak height (V) = 0.00079 ± 0.00002 [Cu(II)] + 0.012 ± 0.022.

3.3.4. Accuracy

To evaluate the accuracy of the micro-FIA analyzer, the recovery percentage (%R) was determined as a measure of the agreement between the copper concentration obtained analytically with the microanalyzer and the true value after the sample was spiked. For this purpose, samples obtained from a copper electrodeposition containing different Cu(II) concentrations ranging from about 500 to 1500 mg L^{-1} were spiked with 500 mg L^{-1} of Cu(II). Each sample was analyzed three times before and after being spiked. The recovery percentage was calculated as % R = ($|Y - X|/500$) × 100%, where X represents the Cu(II) concentration before spiking and Y represents the concentration after the addition of a 500 mg L^{-1}. The results are shown in Table 1.

Table 1. Accuracy results of the samples from copper electrodeposition using the micro-FIA system.

Sample	Concentration of Copper in Samples (mg L^{-1})	Concentration of Copper in Spiked Samples (mg L^{-1})	Recovery (%)
Sample 1	678 ± 18	1193 ± 13	103.0
Sample 2	967 ± 5	1464 ± 11	99.4
Sample 3	1380 ± 9	1882 ± 22	100.4

As shown in Table 1, recoveries of approximately 100% were obtained across the concentration range of 600 to 2000 mg L^{-1}. This indicates that the micro-FIA method developed in the present study is accurate within its linear calibration range.

Table 2 provides a comprehensive overview of the quality parameters for our proposed method. It exhibits satisfactory sensitivity with a wide linear response range from 34 to 2000 mg L^{-1}, ideal for real applications. Furthermore, the method's reproducibility, demonstrated by the standard deviation of measurements across multiple operational days (CV = 3.9–7.4%), underscores the analyzer's reliable and consistent performance in process monitoring.

In order to compare our system with other similar methods, Table S3 shows the characteristics of other flow analysis methods where different reagents are shown [53–60]. The distinctive feature of our analyzer was its extensive linear response range, setting it apart from alternative automated systems. The maximum ranges found in the literature were 1–170 mg L^{-1} [54] and (0.4–40 mg L^{-1}), including studies which also used neocuproine [53]. Both mentioned studies had an LoD of 0.1 mg L^{-1}. However, the lowest LoD found in the literature was 0.005 µg L^{-1}, since the study had a narrow working range (0.05–8 µg L^{-1}) [55]. Obviously, these LoDs are lower than this work (9 mg L^{-1}), since our linear range was 34–2000 mg L^{-1}. In fact, a comparison with the literature supports this, revealing a three-order-of-magnitude difference between the LoD and the maximum concentration of the linear range in our study and the referenced works [53–60]. As regards selectivity, another parameter to compare, the previously mentioned studies

showed good selectivity for determining Cu(II) [53–60]. Nevertheless, among the highly selective methods, one utilized strains of yeast, *S. cerevisiae* [57], while the other employed neocuproine [53], which is the same chelating agent utilized in this study. Finally, in our study both accuracy (101%) and precision (0.3–1.1%) were in accordance with the results presented in other studies [58,59], which reported an accuracy of 99% and a precision of 0.64% and 0.46–0.96%, respectively.

Table 2. Principal parameters of quality of the automatic micro-FIA developed for the determination of Cu(II).

Parameter	Value
Sensitivity (V L mg^{-1})	0.00078 ± 0.00002
Detection limit (mg L^{-1})	9
Quantification limit (mg L^{-1})	34
Linear range (mg L^{-1})	34–2000
Repeatability (CV) (n = 6)	0.3%–1.1%
Reproducibility (CV) (n = 12)	3.9%–7.4%
Selectivity	Not interferences [53]
Sample throughput (h^{-1})	7
Accuracy (R%)	101 ± 2

3.3.5. Real Sample Applications

To assess the applicability of the micro-FIA system, four real media with varying levels of matrix complexity were analyzed as the following: (1) water from Parc de la Agulla in Manresa (Spain), which has a complex composition and high organic matter content; (2) a medium obtained from a bioleaching bioreactor; (3) a leachate obtained from the acid leaching of ion–Li scooter batteries; and (4) a solution obtained from copper electrodeposition. It should be noted that only the third and fourth media contained naturally occurring Cu(II).

The samples were analyzed in triplicate using the developed micro-FIA analyzer, and to contrast the results, they were also analyzed by an atomic absorption spectroscopy reference method.

Least squares linear regression and a paired t-test were used to statistically analyze the results obtained from the two methods. No significant differences were observed at a 95% confidence level. In the least squares linear regression, the slope and intercept were 0.99 ± 0.03 and 6 ± 31, respectively (Figure S3) (R^2 = 0.994; n = 10; 95% confidence level). The calculated t-value was – 0.16, while the tabulated t-value was 2.26 (Table 3). The results of both analytical techniques can be found in Table 3.

In order to demonstrate the real-time monitoring capability of the micro-FIA system, it was connected with an in situ reactor designed for copper oxidation from electrical cables using dissolved Fe(III) present in the reactor. The analyzer successfully tracked the increasing concentration of dissolved copper as it was oxidized from metallic copper during the process. The quantity of copper wires was around 0.9 – 1 g in approximately 1 L of solution and 2400 mg L^{-1} of Fe(III). Measurements were taken at 9-min intervals (frequency analysis, 7 h^{-1}), providing continuous monitoring and automated analysis of the copper concentration.

In order to validate the suitability of the micro-FIA analyzer for the intended purpose, a comparison was made between the analyzer's results and those obtained through batch measurements using atomic absorption spectroscopy used as a reference method. The findings of this comparison are visually presented in Figure 4.

The obtained results demonstrate the capability of the micro-FIA system to monitor the concentrations of copper. The system automatically conducted measurements every 9 min. The results obtained from both methods were compared, and although slight differences were observed, they were not significant enough to attribute solely to the functionality of our system. Minor errors in dilution could cause these variances to appear, which

may have become more pronounced during measurement. The advantages over atomic absorption are that it automatically measures without previous sample pretreatment, no manual sample dilution is required, and the analytical frequency is much higher—thereby minimizing possible dilution errors. Furthermore, the system demonstrates high accuracy and selectivity, as evidenced by the high concordance of results between the two methods.

Table 3. Results from the micro-FIA system of the different samples compared with the results from atomic absorption as the reference method. All samples were analyzed in triplicate. Experimental uncertainty is expressed as the standard deviation.

Sample	[Cu(II)] Added (mg L^{-1})	Copper Concentration Micro-FIA (mg L^{-1})	Copper Concentration Atomic Absorption (mg L^{-1})
Copper electrodeposition	–	763 ± 6	785 ± 32
	–	1278 ± 16	1257 ± 28
	–	1706 ± 18	1698 ± 22
Leaching of ion–Li scooter batteries	–	213 ± 14	218 ± 7
	–	1131 ± 10	1241 ± 28
Water from lake in "Parc de l'agulla"	600	409 ± 6	334 ± 25
	1200	1044 ± 9	1011 ± 23
	1800	1616 ± 10	1619 ± 19
Bioreactor sample	100	65 ± 2	92 ± 2
	1900	1819 ± 25	1814 ± 10

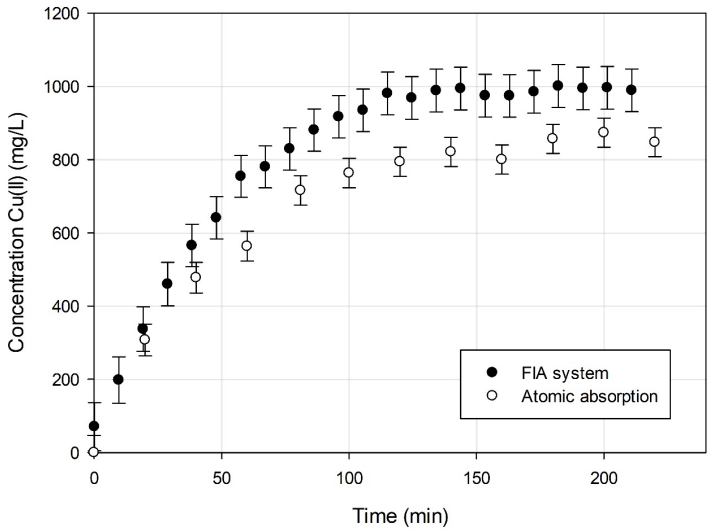

Figure 4. Comparison between online measurements using the novel micro-FIA system (n = 1) and batch determination by the reference method (atomic absorption) (n = 1). Experimental uncertainty was determined for error interpolation.

4. Conclusions

In this work, we developed a modular micro-FIA system using 3D-printed platforms to efficiently monitor high copper concentrations in complex samples with the goal of monitoring a bioleaching process. The system was carefully optimized to allow for the online monitoring of copper over a wide range of concentrations, spanning from 34 to 2000 mg L^{-1}, while maintaining a low detection limit of 9 mg L^{-1}.

Rigorous validation tests were performed to evaluate precision (repeatability and reproducibility), LoD, LoQ, linear response range, accuracy, and applications on real samples. Our results indicate excellent repeatability, with coefficients of variation below C_{vh} over the entire concentration range and were accuracy consistently close to 100%. In

addition, the effectiveness of the system was demonstrated by analyzing four real samples with increasing matrix complexity, obtaining results comparable to those obtained with a reference atomic absorption method, with no significant statistical differences, observed and demonstrating the high selectivity of the method.

Collectively, our findings highlight the numerous benefits that arise from the synergistic integration of miniaturization and continuous flow techniques for the online monitoring of high copper concentrations in complex sample matrices. This innovative approach offers several advantages, including cost reduction through decreased sample and reagent volumes, minimal maintenance requirements, reduced waste disposal, and lower personnel costs. Furthermore, the system's capability for unattended operation over extended durations enhances its practicality and efficiency to monitor real processes.

Finally, this methodology exhibits adaptability and can be readily tailored to detect various analytes of interest, as demonstrated in previous studies. Subsequently, our future investigations will emphasize evaluating the system's capacity for the simultaneous detection of multiple analytes and its potential applicability in the comprehensive monitoring of bioleaching bioreactors.

Supplementary Materials: The following supporting information can be downloaded at: https://www.mdpi.com/article/10.3390/chemosensors12070119/s1, Figure S1: (A) CAD of platform 1 formed by a hydroxylamine mixer module connected to a diluter module via a Tesla valve. (B) Dimensional labelling of the hydroxylamine mixer with a height of 0.5 mm. (C) Dimensional labeling of the diluter [47] with a height of 0.75 mm. The units for the dimensions are in millimeters. Figure S2: Dimensional labeling of the disperser [47] with a height of 1 mm with Tesla valve in CAD. The units for the dimensions are in millimeters. Table S1: Results of repeatability of the modular micro-FIA system. Table S2: Results of reproducibility of the modular micro-FIA system. Figure S3: Linear regression test to compare the reference method (atomic absorption) and the proposed micro-FIA analyzer. Table S3: An overview on better reported optical methods for the determination of Cu(II).

Author Contributions: Conceptualization, M.B., C.L.-L. and A.D.D.; methodology, D.R., C.L.-L. and M.B.; validation, D.R. and C.L.-L.; investigation, D.R.; resources, A.D.D. and M.B.; data curation, D.R., C.L.-L. and M.B; writing—original draft preparation, D.R. and C.L.-L.; writing—review and editing, D.R., C.L.-L., A.D.D. and M.B.; visualization, A.D.D. and M.B.; supervision, C.L.-L. and M.B.; project administration, A.D.D.; funding acquisition, A.D.D. All authors have read and agreed to the published version of the manuscript.

Funding: Project BIOMETAL PID2020-117520RA-I00 funded by MCIN/AEI/10.13039/501100011033 and BIOCOLI ACE034/21/000044 funded by ACCIÓ.

Institutional Review Board Statement: Not applicable.

Informed Consent Statement: Not applicable.

Data Availability Statement: The data presented in this study are available upon request from the corresponding author. The data are not publicly available because the repository that was used to keep the data was a private one provided by the university.

Acknowledgments: The authors gratefully acknowledge the UPC for the financial support of a predoctoral grant FPU-UPC, with the collaboration of Banco de Santander.

Conflicts of Interest: The authors declare no conflicts of interest.

References

1. Laurmaa, V.; Kers, J.; Tall, K.; Mikli, V.; Goljandin, D.; Vilsaar, K.; Peetsalu, P.; Saarna, M.; Tarbe, R.; Zhang, L. *Mechanical Recycling of Electronic Wastes for Materials Recovery*; John Wiley & Sons, Inc.: Hoboken, NJ, USA, 2011; pp. 3–10. [CrossRef]
2. Dorado, A.D.; Solé, M.; Lao, C.; Alfonso, P.; Gamisans, X. Effect of PH and Fe(III) Ions on Chalcopyrite Bioleaching by an Adapted Consortium from Biogas Sweetening. *Miner. Eng.* **2012**, *39*, 36–38. [CrossRef]
3. Dorado Castaño, A.D.; Gamisans Noguera, X.; Solé Sardans, M.; Lao Luque, C.; Benzal Montes, E. Method for the Biological Recovery of Metals in Electric and Electronic Waste. Patent WO2019206755A1, 31 October 2019.
4. Brierley, C.L. Bacterial Succession in Bioheap Leaching. *Process Metall.* **1999**, *9*, 91–97. [CrossRef]

5. Benzal, E.; Solé, M.; Lao, C.; Gamisans, X.; Dorado, A.D. Elemental Copper Recovery from E-Wastes Mediated with a Two-Step Bioleaching Process. *Waste Biomass Valorization* **2020**, *11*, 5457–5465. [CrossRef]
6. Benzal, E.; Cano, A.; Solé, M.; Lao-Luque, C.; Gamisans, X.; Dorado, A.D. Copper Recovery from PCBs by Acidithiobacillus Ferrooxidans: Toxicity of Bioleached Metals on Biological Activity. *Waste Biomass Valorization* **2020**, *11*, 5483–5492. [CrossRef]
7. Zhan, Y.; Yang, M.; Zhang, S.; Zhao, D.; Duan, J.; Wang, W.; Yan, L. Iron and Sulfur Oxidation Pathways of Acidithiobacillus Ferrooxidans. *World J. Microbiol. Biotechnol.* **2019**, *35*, 60. [CrossRef]
8. Ma, L.; Liu, G.; Pu, S.; Ding, H.; Li, G. A Highly Selective Fluorescent Chemosensor for Cu^{2+} Based on a New Diarylethene with Triazole-Linked Fluorescein. *Tetrahedron* **2016**, *72*, 985–991. [CrossRef]
9. Su, Y.; Shi, B.; Liao, S.; Qin, Y.; Zhang, L.; Huang, M.; Zhao, S. Facile Preparation of Fluorescent Polydihydroxyphenylalanine Nanoparticles for Label-Free Detection of Copper Ions. *Sens. Actuators B Chem.* **2016**, *225*, 334–339. [CrossRef]
10. Gupta, V.K.; Singh, L.P.; Singh, R.; Upadhyay, N.; Kaur, S.P.; Sethi, B. A Novel Copper (II) Selective Sensor Based on Dimethyl 4, 4′ (o-Phenylene) Bis(3-Thioallophanate) in PVC Matrix. *J. Mol. Liq.* **2012**, *174*, 11–16. [CrossRef]
11. Munoz, R.A.A.; Angnes, L. Simultaneous Determination of Copper and Lead in Ethanol Fuel by Anodic Stripping Voltammetry. *Microchem. J.* **2004**, *77*, 157–162. [CrossRef]
12. Kitte, S.A.; Li, S.; Nsabimana, A.; Gao, W.; Lai, J.; Liu, Z.; Xu, G. Stainless Steel Electrode for Simultaneous Stripping Analysis of Cd(II), Pb(II), Cu(II) and Hg(II). *Talanta* **2019**, *191*, 485–490. [CrossRef] [PubMed]
13. Osipova, E.A.; Sladkov, V.E.; Kamenev, A.I.; Shkinev, V.M.; Geckeler, K.E. Determination of Ag(I), Hg(II), Cu(II), Pb(II), Cd(II) by Stripping Voltammetry in Aqueous Solutions Using Complexing Polymers in Conjunction with Membrane Filtration. *Anal. Chim. Acta* **2000**, *404*, 231–240. [CrossRef]
14. Yang, W.; Jaramillo, D.; Gooding, J.J.; Hibbert, D.B.; Zhang, R.; Willett, G.D.; Fisher, K.J. Sub-Ppt Detection Limits for Copper Ions with Gly-Gly-His Modified Electrodes. *Chem. Commun.* **2001**, *1*, 1982–1983. [CrossRef]
15. Mohadesi, A.; Taher, M.A. Voltammetric Determination of Cu(II) in Natural Waters and Human Hair at a Meso-2,3-Dimercaptosuccinic Acid Self-Assembled Gold Electrode. *Talanta* **2007**, *72*, 95–100. [CrossRef]
16. Jain, A.K.; Gupta, V.K.; Sahoo, B.B.; Singh, L.P. Copper(II)-Selective Electrodes Based on Macrocyclic Compounds. *Anal. Proc.* **1995**, *32*, 99–101. [CrossRef]
17. Gupta, V.K.; Ganjali, M.R.; Norouzi, P.; Khani, H.; Nayak, A.; Agarwal, S. Electrochemical Analysis of Some Toxic Metals by Ion–Selective Electrodes. *Crit. Rev. Anal. Chem.* **2011**, *41*, 282–313. [CrossRef]
18. Hsiang, M.C.; Sung, Y.H.; Huang, S. Da Direct and Simultaneous Determination of Arsenic, Manganese, Cobalt and Nickel in Urine with a Multielement Graphite Furnace Atomic Absorption Spectrometer. *Talanta* **2004**, *62*, 791–799. [CrossRef]
19. Cassella, R.J.; Magalhães, O.I.B.; Couto, M.T.; Lima, E.L.S.; Neves, M.A.F.S.; Coutinho, F.M.B. Synthesis and Application of a Functionalized Resin for Flow Injection/F AAS Copper Determination in Waters. *Talanta* **2005**, *67*, 121–128. [CrossRef]
20. Mashhadizadeh, M.H.; Pesteh, M.; Talakesh, M.; Sheikhshoaie, I.; Ardakani, M.M.; Karimi, M.A. Solid Phase Extraction of Copper (II) by Sorption on Octadecyl Silica Membrane Disk Modified with a New Schiff Base and Determination with Atomic Absorption Spectrometry. *Spectrochim. Acta Part B At. Spectrosc.* **2008**, *63*, 885–888. [CrossRef]
21. Chrastný, V.; Komárek, M. *Copper Determination Using ICP-MS with Hexapole Collision Cell*; Walter de Gruyter: Berlin, Germany, 2009; Volume 63, pp. 512–519. [CrossRef]
22. Wu, Q.; He, J.; Meng, H.; Wang, Y.; Zhang, Y.; Li, H.; Feng, L. A Paper-Based Microfluidic Analytical Device Combined with Home-Made SPE Column for the Colorimetric Determination of Copper(II) Ion. *Talanta* **2019**, *204*, 518–524. [CrossRef] [PubMed]
23. Cotton, D.H.; Jenkins, D.R. The Determination of Very Low Concentrations of Copper, Iron and Lead in Hydrocarbon Fuels by Atomic Fluorescence Spectrometry. *Spectrochim. Acta Part B At. Spectrosc.* **1970**, *25*, 283–288. [CrossRef]
24. Hu, Q.; Yang, G.; Zhao, Y.; Yin, J. Determination of Copper, Nickel, Cobalt, Silver, Lead, Cadmium, and Mercury Ions in Water by Solid-Phase Extraction and the RP-HPLC with UV-Vis Detection. *Anal. Bioanal. Chem.* **2003**, *375*, 831–835. [CrossRef]
25. Xiong, X.; Jiang, T.; Zhou, R.; Wang, S.; Zou, W.; Zhu, Z. Microwave Plasma Torch Mass Spectrometry for the Direct Detection of Copper and Molybdenum Ions in Aqueous Liquids. *J. Mass Spectrom.* **2016**, *51*, 369–377. [CrossRef]
26. Harvey, D.; Frederick, S.G. *The Copper Reagents: Cuproine, Neocuproine, Bathocuproine*, 1st ed.; Frederick, S.G., Ed.; Chemical Company: Columbus, OH, USA, 1958.
27. Pourbasheer, E.; Morsali, S.; Banaei, A.; Aghabalazadeh, S.; Ganjali, M.R.; Norouzi, P. Design of a Novel Optical Sensor for Determination of Trace Amounts of Copper by UV/Vis Spectrophotometry in the Real Samples. *J. Ind. Eng. Chem.* **2015**, *26*, 370–374. [CrossRef]
28. Gahler, A.R. Colorimetric Determination of Copper with Neo-Cuproine. *Anal. Chem.* **1954**, *26*, 577–579. [CrossRef]
29. Ogawa, T.; Hata, N.; Taguchi, S. Technical Note Selective a N D Sensitive Spectrophotometric Determination of Copper in Water After Collection of Its Bathocuproine Complex on an Organic-Solvent-Soluble Membrane Filter. *Water Res.* **1989**, *23*, 933–936.
30. Frederick Smith, G.; McCurdy, W.H. New Specific in Spectrophotometric Determination of Copper. *Anal. Chem.* **1952**, *24*, 371–373.
31. Smith, G.F.; Wilkins, D.H. New Colorimetric Reagent Specific for Cooper. *Anal. Chem.* **1953**, *25*, 510–511. [CrossRef]
32. Moffett, J.W.; Zika, R.G.; Petasne, R.G. Evaluation of Bathocuproine for the Spectro-Photometric Determination of Copper(I) in Copper Redox Studies with Applications in Studies of Natural Waters. *Anal. Chim. Acta* **1985**, *175*, 171–179. [CrossRef]
33. Hoste, J.; Eeckhout, J.; Gillis, J. Spectrophotometric Determination of Copper with Cuproine. *Anal. Chim. Acta* **1953**, *9*, 263–274. [CrossRef]

34. Rajput, N.; Kadam, V.; Devi, S. Spectrophotometric Determination of Copper (II) Using Cupron in the Presence of Brij 35. *Indian J. Chem.* **1994**, *33A*, 88–90.
35. Wiberley, S.E.; Dunleavy, R.A.; Harley, J.H. Rapid Photometric Determination of Copper in Ferrous Alloys. *Anal. Chem.* **1950**, *22*, 170–172. [CrossRef]
36. Thongkam, T.; Apilux, A.; Tusai, T.; Parnklang, T.; Kladsomboon, S. Thy-AuNP-AgNP Hybrid Systems for Colorimetric Determination of Copper (II) Ions Using UV-Vis Spectroscopy and Smartphone-Based Detection. *Nanomaterials* **2022**, *12*, 1449. [CrossRef]
37. Reshetnyak, E.A.; Ivchenko, N.V.; Nikitina, N.A. Photometric Determination of Aqueous Cobalt (II), Nickel (II), Copper (II) and Iron (III) with 1-Nitroso-2-Naphthol-3,6-Disulfonic Acid Disodium Salt in Gelatin Films. *Cent. Eur. J. Chem.* **2012**, *10*, 1617–1623. [CrossRef]
38. Kang, J.H.; Lee, S.Y.; Ahn, H.M.; Kim, C. Sequential Detection of Copper(II) and Cyanide by a Simple Colorimetric Chemosensor. *Inorg. Chem. Commun.* **2016**, *74*, 62–65. [CrossRef]
39. Zhou, F.; Li, C.; Zhu, H.; Li, Y. Simultaneous Determination of Trace Metal Ions in Industrial Wastewater Based on UV–Vis Spectrometry. *Optik* **2019**, *176*, 512–517. [CrossRef]
40. Turkoglu, O.; Soylak, M. Spectrophotometric Determination of Copper in Natural Waters and Pharmaceutical Samples with Chloro(Phenyl) Glyoxime. *J. Chin. Chem. Soc.* **2005**, *52*, 575–579. [CrossRef]
41. Zhou, F.; Li, C.; Zhu, H.; Li, Y. A Novel Method for Simultaneous Determination of Zinc, Nickel, Cobalt and Copper Based on UV–Vis Spectrometry. *Optik* **2019**, *182*, 58–64. [CrossRef]
42. Aydin, Z.; Keles, M. Colorimetric Detection of Copper(II) Ions Using Schiff-Base Derivatives. *ChemistrySelect* **2020**, *5*, 7375–7381. [CrossRef]
43. Shen, Q.; Li, W.; Tang, S.; Hu, Y.; Nie, Z.; Huang, Y.; Yao, S. A Simple "Clickable" Biosensor for Colorimetric Detection of Copper(II) Ions Based on Unmodified Gold Nanoparticles. *Biosens. Bioelectron.* **2013**, *41*, 663–668. [CrossRef]
44. Rumori, P.; Cerdà, V. Reversed Flow Injection and Sandwich Sequential Injection Methods for the Spectrophotometric Determination of Copper(II) with Cuprizone. *Anal. Chim. Acta* **2003**, *486*, 227–235. [CrossRef]
45. León, L.; Carbajo, J.; Maraver, J.J.; Mozo, J.D. Sequential Determination of Mono- and Divalent Copper in Water by Flow-Injection Analysis. *J. Electrochem. Soc.* **2014**, *161*, H183–H188. [CrossRef]
46. Galera, I. Estudi Per a La Conversió a Continu Del Procés De Biolixiviació a Escala Pilot, EPSEM. Bachelor's Thesis, Universitat Politècnica de Catalunya, Barcelona, Spain, 2018.
47. Ricart, D.; Dorado, A.D.; Lao-Luque, C.; Baeza, M. Microflow Injection Analysis Based on Modular 3D Platforms and Colorimetric Detection for Fe(III) Monitoring in a Wide Concentration Range. *Microchim. Acta* **2023**, *191*, 3. [CrossRef]
48. Baeza, M.; Montesinos, J.L.; Alonso, J.; Bartrolí, J. Simple Modeling of the Physical Sample Dispersion Process in Rectangular Meso (Micro) Channels with Pressure-Driven Flows. *Anal. Bioanal. Chem.* **2009**, *393*, 1233–1243. [CrossRef]
49. Nikola Tesla Valvular Conduit. U.S. Patent US1329559A, 3 February 1920.
50. Abdelwahed, M.; Chorfi, N.; Malek, R. Reconstruction of Tesla Micro-Valve Using Topological Sensitivity Analysis. *Adv. Nonlinear Anal.* **2019**, *9*, 567–590. [CrossRef]
51. Horwitz, W. Evaluation of Analytical Methods Used for Regulation of Foods and Drugs. *Anal. Chem.* **1982**, *54*, 67–76. [CrossRef]
52. McNaught, A.D.; Wilkinson, A. *Compendium of Chemical Terminology*, 2nd ed.; IUPAC Nomenclature Books Series ("Color Books"); Blackwell Science: Oxford, UK, 1997; ISBN 0-86542-6848.
53. Farhood, A.S.; Taha, D.N. A New Flow Injection System with Merging-Zone Technique for the Determination of Copper(II) by Neocuproine Reagent in Aqueous Solution. *Indones. J. Chem.* **2022**, *22*, 770–779. [CrossRef]
54. Ali, K.J.; Abdul, N.; Hameed, R. Determination of Copper (II) by Glycine in Flow Injection and Sequential Injection Techniques. *Acta Chim. Pharm. Indica* **2014**, *4*, 157–169.
55. Wei, J.; Teshima, N.; Ohno, S.; Sakai, T. Catalytic Flow-Injection Determination of Sub-Ppb Copper (II) Using the Redox Reaction of Cysteine with Iron (III) in the Presence of TPTZ. *Anal. Sci.* **2003**, *19*, 731–735. [CrossRef]
56. Zenki, M.; Iwadou, Y.; Yokoyama, T. Flow-Injection Analysis of Copper(II) with PAR in the Presence of EDTA. *Anal. Sci.* **2002**, *18*, 1077–1079. [CrossRef]
57. Tag, K.; Riedel, K.; Bauer, H.J.; Hanke, G.; Baronian, K.H.R.; Kunze, G. Amperometric Detection of Cu^{2+} by Yeast Biosensors Using Flow Injection Analysis (FIA). *Sens. Actuators B Chem.* **2007**, *122*, 403–409. [CrossRef]
58. Asan, A.; Isildak, I.; Andac, M.; Yilmaz, F. A Simple and Selective Flow-Injection Spectrophotometric Determination of Copper(II) by Using Acetylsalicylhydroxamic Acid. *Talanta* **2003**, *60*, 861–866. [CrossRef] [PubMed]
59. Ohno, S.; Tanaka, M.; Teshima, N.; Sakai, T. Successive Determination of Copper and Iron by a Flow Injection-Catalytic Photometric Method Using a Serial Flow Cell. *Anal. Sci.* **2004**, *20*, 171–175. [CrossRef] [PubMed]
60. Lima, J.L.F.C.; Delerue-Matos, C.; Vaz, M.C.V.F. Automation of Iron and Copper Determination in Milks Using FIA Systems and Colourimetric Detection. *Food Chem.* **1998**, *62*, 117–121. [CrossRef]

Disclaimer/Publisher's Note: The statements, opinions and data contained in all publications are solely those of the individual author(s) and contributor(s) and not of MDPI and/or the editor(s). MDPI and/or the editor(s) disclaim responsibility for any injury to people or property resulting from any ideas, methods, instructions or products referred to in the content.